Role of the Geometry, Restricted Rotations and Solvents on the Computed 2,2′-Diphenyl-1-picrylhydrazyl Hyperfine Tensors

Saba M. Mattar* and Jacob Sanford

Department of Chemistry and Centre for Laser, Atomic and Molecular Sciences, University of New Brunswick, Fredericton, NB, Canada E3B 6E2

Received: August 3, 2008; Revised Manuscript Received: September 17, 2008

The nuclear hyperfine tensor (**A**) components of the 2,2′-diphenyl-1-picrylhydrazyl neutral radical are computed using the UB1LYP hybrid density functional method. Solvent interactions via hydrogen bonding are found to play a crucial role in the position of the two phenyl rings relative to the picryl moiety. Under these conditions, the calculated isotropic hyperfine tensor components of the N_1 and N_2 hydrazyl backbone are within ∼1.3 Gauss (G) of the experimental values determined by EPR and ENDOR spectroscopy. Just as important are the effects of restricted rotations of the phenyl rings on these tensors. Rotational averaging using a Maxwell−Boltzmann type distribution improves the agreement between theory and experiment to less than 1.0 G. In addition, rotational averaging of the twelve isotropic proton coupling constants has also been performed. They come within 0.3 G of the experimental values. Thus, for the first time, all the nuclear hyperfine tensor components of this large class of molecules are accurately calculated without resorting to post Hartree−Fock techniques.

1. Introduction

The neutral free radical 2,2′-diphenyl-1-picrylhydrazyl (DPPH•), shown in Figure 1, was discovered approximately 80 years ago.[1] It is a stable radical and has been used as a standard in electron paramagnetic resonance (EPR) spectroscopy at X-band (9 GHz)[2,3] and recently at higher frequencies (465 GHz).[4,5] It has also gained popularity due to its ability to scavenge other radicals.[6]

DPPH• was the first radical to exhibit hyperfine splittings in an EPR spectrum.[7] It was later determined that its N_1 and N_2 atoms were inequivalent and their isotropic hyperfine splittings, $a^{iso}(^{14}N_1)$ and $a^{iso}(^{14}N_2)$, were different.[8]

The DPPH• spectral parameters were determined when it was doped in single crystals[9] and in randomly oriented solids.[10,11] The effects of different solvents on the DPPH• radical reactivity, spin density distributions and nuclear hyperfine coupling constants were first studied in 1963.[12] Later, Valgimigli et al. also investigated the kinetic solvent effects on the reactivity of DPPH•.[13] To differentiate between the N_1 and N_2 atoms, they followed the earlier suggestion of Deal and Koski[8] and synthesized DPPH• with isotopically enriched $^{15}N_1$. They monitored the magnitude of $a^{iso}(N_1)$ and $a^{iso}(N_2)$ in different solvents. The ratio of the $a^{iso}(^{14}N_1)/a^{iso}(^{14}N_2)$was found to vary between 1.17 and 1.23.[13] Thus, it is important to understand the mechanism by which the different solvents affect the reactivity of DPPH• and the magnitude of its hyperfine coupling constants.

All the nuclei of DPPH• are magnetically inequivalent. This is due to its low C_1 molecular symmetry.[14] However, because of rotational and vibrational motions, some averaging is expected to occur. In their seminal electron nuclear double resonance (ENDOR) studies, Dalal et al. show that, even at −5 °C, the phenyl protons appeared to be magnetically equivalent and the picryl protons were inequivalent.[15−17] Therefore, it was suggested that the phenyl groups may rapidly rotate and average out the inequivalency of their protons.[17] They also did not rule out the fact that "A non symmetry position has a much smaller effect on the hyperfine couplings of the phenyl protons as compared to those of the picryl protons".[17] These results indicate that rotational averaging must influence the appearance of the ENDOR spectrum of this molecule.

Ideally, it is important to correlate the observed magnetic properties and spin Hamiltonian parameters with those calculated by a reliable computational method. A good agreement between theory and experiment enables one to relate the radical's electronic structure and geometry to its bonding properties and reactivity. Although the anisotropic nuclear hyperfine tensor components of a particular nucleus can easily be computed at the unrestricted Hartree−Fock (UHF) level,[18−20] the corresponding isotropic hyperfine tensor component remains one of the most difficult properties to calculate. The quality of the calculated wave function must be very high, requiring post UHF procedures such as multireference configuration interaction.[19−21]

Hybrid density functional (HDF) techniques have been very successful in computing the electronic structure, optimal geometries and vibrational frequencies of molecules with ground states that may be approximated by a single determinant.[22,23] The UB1LYP and PBE0 HDFs have recently been used with moderate basis sets such as, 6-31G*, EPR-II and EPR-III to accurately compute the a^{iso} values of organic free radicals containing H, C, N, and O atoms.[24−28] The UB1LYP and PBE0 HDFs also have the additional advantage of containing no adjustable parameters

During the past few years, we have been able to accurately compute the hyperfine coupling constants using the unrestricted-Beck-1-parameter Lee−Yang−Parr (UB1LYP) HDF method and the EPR-II basis sets of Barone.[29] We found that the accuracy remains essentially the same as the radicals increase in size. Excellent results have been calculated in a range of molecular sizes—from free radicals that contain only hydrogen, carbon and oxygen, such as DTBN[30] and TEMPONE,[28] to, more

* Corresponding author. E-mail: mattar@unb.ca. Telephone: +1 (506) 447 3091. Fax: +1 (506) 453 4981.

10.1021/jp806919k CCC: $40.75
Published on Web 10/17/2008

recently, larger inorganic species that include nitrogen, fluorine and sulfur and copper.[31−33] These positive results have encouraged us to compute the DPPH• nitrogen and hydrogen isotropic hyperfine coupling constants, a^{iso}(N)and a^{iso}(H). The computations are challenging and time-consuming, as DPPH• is a large radical that contains 41 atoms. Due to the molecule's inherent nonrigid character, solvent−solute interactions are expected to influence the relative orientation of its phenyl and picryl functional groups. These, in turn, will affect its $a^{iso}(N)$and $a^{iso}(H)$ values. Consequently, meaningful and rigorous computations for this radical, that explain the experimental spectra, must take into account these solvent effects, phenyl ring rotations and equivalency of the NO_2 groups of the picryl ring.

The first calculations of the electronic structure of DPPH• were carried out in 1966 and used a Hückel molecular orbital (MO) method.[34] Due to the approximate semiempirical nature of this method, no reliable correlations with the experimental properties and spectra could be made. Gubanov et al. improved on the previous calculations slightly by starting off with a semiempirical self-consistent field (SCF) linear combination of atomic orbital (LCAO) method.[35] However, the calculations were performed assuming that the DPPH• radical was planar.[11] No theoretical geometry optimizations were carried out and the atomic coordinates were not taken from the existing X-ray single crystal structure data.[36−38]

Significant effort and a large amount of research have been spent in the calculation of **A** tensor components. Recently, **g** tensors have also been accurately computed, using ab initio, density functional, hybrid density functionals, and spectroscopy oriented configuration interaction. Therefore, one is now in a position calculate the magnitudes of *all* the spin Hamiltonian tensor components. Recently, we have accurately determined the effects of restricted rotations and solvents on the calculated DPPH• **g** tensors.[39] As a continuation, the present article deals with the corresponding **A** tensor components. From both of these **g** and **A** tensors, the effects of magnetically inequivalent DPPH• atoms on its EPR and ENDOR spectra may be fully assessed and calculated.

2. Experimental and Computational Details

The ORCA[40] and GAUSSIAN 03[41] programs were used for the geometry optimizations, electronic structure, **g** and **A** tensor computations. The radical was optimized in the gas phase and also when interacting with a number of solvent molecules using the PM3 method. Methanol is the smallest solvent molecule that will dissolve DPPH•. Thus, to minimize the computational times, it was selected as the solvent of choice. A set of supermolecules were formed by hydrogen bonding DPPH• with one to six methanol molecules. They were individually geometry optimized until the sum of the energy gradients was less than 0.0005 kcal $Å^{-1}$ mol^{-1}. The resulting optimal geometries were checked to ensure that they did not possess any imaginary vibrational frequencies that are characteristic of saddle points or transition states on the energy surfaces.

The optimized geometries were then used to compute the **A** tensor components employing Barone's EPR-II basis set and the UB1LYP HDF method.[24,29,42,43] This will be hereafter referred to as the UB1LYP/EPR-II method. The EPR-II basis set was chosen for the computation of the hyperfine **A** tensors because of its very tight s functions.[29]

The effects of the methanol solvent, without forming a supermolecule, were also investigated using Tomasi's polarized continuum method (PCM) method that is abbreviated as (UB1LYP-PCM/EPR-II).[39,44,45] In this technique, implemented by the GAUSSIAN 03 program, the molecule is located in a solvent cavity, constructed from a series of interlocking spheres, using the methanol dielectric constant, $\varepsilon = 32.63$. The COSMO method[46] was employed when performing calculations with the ORCA program.

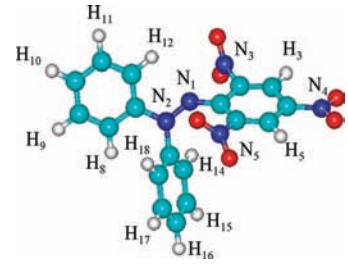

Figure 1. Atomic numbering of 2,2′-diphenyl-1-picrylhydrazyl radical. For simplicity, only the N and H atoms have been labeled. Hydrogen atoms adopt their numbering from the adjacent (parent) carbon atoms.

The EPR spectra were recorded using a modified Varian E104 continuous wave (CW) spectrometer.[30,47−49] The spectrometer utilized a DR/TE_{102} dielectric resonator instead of a regular TE_{102} cavity.[49] This increases its sensitivity by a factor of 25 and allows the use of very small modulation amplitudes, which are essential in resolving narrow hyperfine splittings. The magnetic field was modulated by a 50 kHz sine wave and the second harmonic of the EPR signal was detected. The spectra were digitized via a National Instruments ATMIO16E10 data acquisition board. The magnetic field was measured using a Bell 640 differential Gauss meter. The microwave power was monitored with an HP 432C digital power meter equipped with an HP 478A thermistor power head.

The DPPH• radical was purchased from Eastman Organic Chemicals Inc. To maximize the resolution of the DPPH• hyperfine splittings, a 0.3 mM solution in benzene-d_6 was prepared and purged with oxygen-free dry nitrogen gas for 15 min before the spectra was recorded.

3. Results and Discussion

3.1. Optimal Gas Phase Geometry and Electronic Ground State. Partial optimization of the DPPH• radical was performed while keeping the backbone of the phenyl and picryl rings planar. The optimized geometry, shown in Figure 1, is nonplanar and very close to that determined by X-ray crystallography.[38] The largest difference between the computed and experimental geometries is approximately 10 degrees. It involves the torsion angle between the *p*-NO_2 picryl group and its ring plane. This is not surprising because the gas phase results do not take into account the packing effects that could occur in the experimental X-ray structure.

The nonplanar DPPH• radical has one unpaired electron and a $^2A_1$ ground state. Because of it is C_1 symmetry, all its atoms are spatially and magnetically inequivalent.[14] The unpaired electron density, although mainly located on the central nitrogen atoms, is nevertheless delocalized over the entire molecule. Assuming no rotational averaging, the nuclear hyperfine interactions from the twelve ^1H and five ^{14}N naturally occurring inequivalent isotopes generate

$$\prod_{i=1}^{12}[2I(^1H_i)+1]\prod_{j=1}^{5}[2I(^{14}N_j)+1] = 995{,}328$$

EPR lines, as shown in Figure 2. These enormous numbers of closely spaced lines overlap with each other causing inhomogeneous line shape broadening and partially resolved spectra.

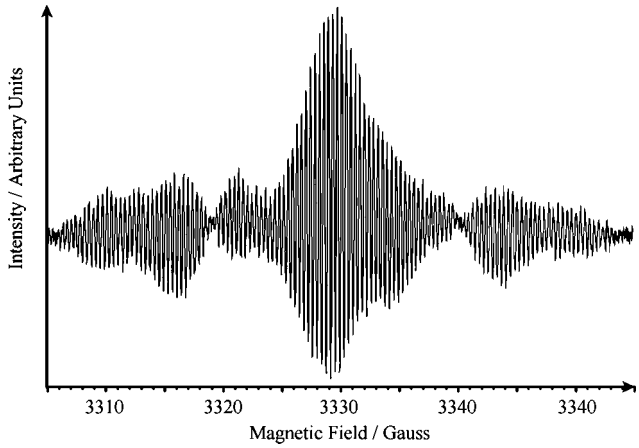

Figure 2. Second derivative electron paramagnetic resonance of 0.3 mM DPPH• in benzene-d_6 saturated with dry oxygen-free nitrogen gas. Conditions: frequency 9.0362 GHz, power 73 μW, modulation amplitude 0.063 G, modulation frequency 50 KHz, time constant 0.016 s, scan speed 0.1G/s and number of averages 100.

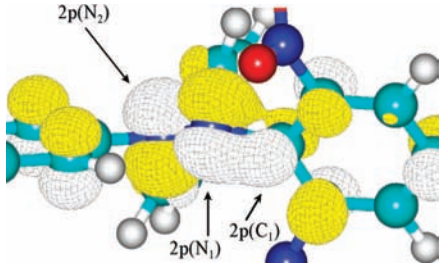

Figure 3. Three-dimensional plot of the **DPPH•** singly occupied molecular orbital (SOMO) in the vicinity of the $N_2-N_1-C_1$ atoms. The yellow surfaces indicate positive lobes, and the gray surfaces signify negative lobes. The 2p orbital components of the N_1, N_2 and C_1 atoms are indicated by the arrows.

While rotational averaging along certain bonds is possible and reduces the number of EPR lines, they are still too numerous to be adequately assigned.

Figure 3 shows the singly occupied molecular orbital (SOMO) in the vicinity of the N_1-N_2 hydrazyl moiety. The Lowdin bond orders between the N_2 and the phenyl rings are 1.05 and 1.09.[39] This indicates that they are essentially single bonds and, barring any other steric influence, free rotation of the phenyl rings may occur. However, the bond between N_1 and C_1 of the picryl ring has an order of 1.50. This partial double bond character would infer that free rotation of the picryl ring is doubtful. The N_1-N_2 bond order is 1.45[39] and very close to that of the N_1-C_1 bond. Thus, the $N_2-N_1-C_1$ fragment has partial double bond character spanning its three centers.

Inspection of the SOMO in Figure 3 shows π bonding character between N_1 and C_1, and it is antibonding between the $2p(N_1)$ and $2p(N_2)$ atomic orbitals. The N_1-C_1 bond is twisted but still maintains some double bond character. The net spin density from all electrons at N_1 is greater than that at N_2 as indicated by the larger value of its hyperfine coupling constant, $a^{iso}(^{14}N_1)$.

3.2. Calculation of the Nitrogen Nuclear Hyperfine Coupling Constants. The experimental and computed hyperfine coupling constants, using the UB1LYP method with the EPR-II basis set, are listed in Table 1. The computations were carried out in the gas phase and with a variety of solvents, using UB1LYP-PCM/EPR-II. These structures were geometry optimized, employing the PM3 approximation, to an energy minimum. The resultant geometry was then used in a B1LYP calculation to determine the hyperfine tensor components for each atom.

TABLE 1: N_1 and N_2 Isotropic Hyperfine Coupling Constants[a] in Different Solvents

solvent	$a^{iso}(^{14}N_1)$	$a^{iso}(^{14}N_2)$	ΔE^b	dielectric const
	Experimental Values[c]			
CCl_4	9.77	7.94		
DMSO	9.30	8.10		
methanol	9.54	8.10		
acetonitrile	9.80	7.94		
benzene	9.77	7.94		
ethanol	9.55	8.11		
	Computed Values/UB1LYP			
gas phase	11.23	6.64		
PCM/CCl4	10.93	6.59	6.67	2.23
PCM/DMSO	10.50	7.11	3.78	46.70
PCM/methanol	10.20	7.27	−7.54	32.63
PCM/acetonitrile	10.50	7.11	9.37	36.64
PCM/benzene	10.93	6.86	5.36	2.25
PCM/ethanol	10.22	7.24	−2.41	24.53
DPPH•-$(MeOH)_1$	9.36	6.80	−5.04	32.63
DPPH•-$(MeOH)_2$	8.41	7.52	−7.69	32.63
DPPH•-$(MeOH)_3$	9.64	6.86	−10.75	32.63
DPPH•-$(MeOH)_4$	9.38	8.21	−12.58	32.63
DPPH•-$(MeOH)_6$	9.49	8.61	−15.40	32.63

[a] Values in G. [b] Total energy change due to solvation or hydrogen bonding in kcal/mol [c] From Valgimigli et al.[13]

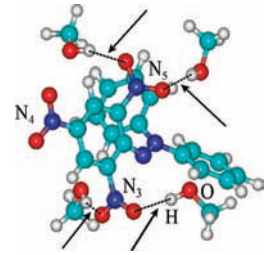

Figure 4. Supermolecule formed by DPPH• hydrogen bonding with four methanol molecules, DPPH•−$(MeOH)_4$. Hydrogen bonding between H atoms of the methanol hydroxyl groups and the two *o*-picryl NO_2 oxygens are indicated by dashed lines.

Table 1 shows that the influence of solvents on $a^{iso}(^{14}N_1)$ and $a^{iso}(^{14}N_2)$, when computed by the PCM method. These effects are small and are scattered within the computational error range. This agrees with the data previously published by Valgimigli et al.[13] However, the table also indicates that the calculated $a^{iso}(^{14}N_1)$ and $a^{iso}(^{14}N_2)$, values come as close as 0.7 G (in ethanol) and as far as 1.3 G (in carbon tetrachloride) to their experimental counter

One of the main deficiencies of the PCM model is its inability to describe hydrogen bonding. Consequently, it has recently been shown that taking into account the direct interaction of the solvent molecules with radicals, via hydrogen bonding, results in improved calculated hyperfine and **g** tensors.[50,51] Accordingly, the effects of methanol as a solvent were also investigated by constructing a supermolecule made up of DPPH• and a number of hydrogen bonded methanols. These results are listed in the last five rows of Table 1. They indicate that it takes at least four methanol molecules to hydrogen bond with the radical and position the three DPPH• rings appropriately. This configuration, DPPH•−$(MeOH)_4$, is illustrated in Figure 4 and results in $a^{iso}(^{14}N_1)$ and $a^{iso}(^{14}N_2)$ values that are the closest to the experimental ones. The differences between the experimental and computed values are less than 0.16 G.

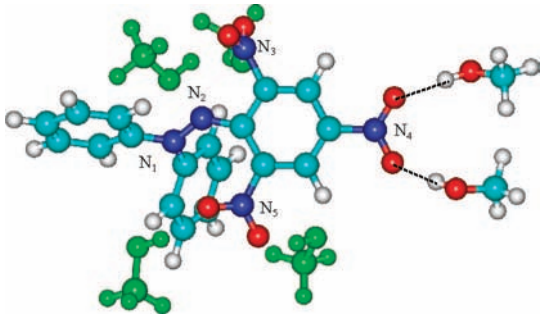

Figure 5. Optimized geometry as a result of adding two extra methanols to form DPPH•−(MeOH)$_6$. Note that the two extra methanol hydroxyl H atoms interact with the picryl *p*-NO_2 oxygens. For clarity, the first four methanols, originally shown in Figure 4, are green.

3.3. Nature of DPPH•−Solvent Interactions. Valgimigli et al. studied the reactivity and net spin density distribution of DPPH• in various solvents by EPR spectroscopy.[13] Except for *tert*-butyl alcohol, the reactivity was found to be independent of the solvent. Several theories were put forward to explain these observations. However, the authors felt that none was totally satisfactory.[13] The geometry optimized [DPPH•−(methanol)$_n$] supermolecules computed in this study may be used to shed additional light on the nature of these DPPH•−solvent interactions.

As an example, Figure 4 depicts the interaction of DPPH• with four methanol molecules. These interactions are mainly with the outer surface of the DPPH• and do not directly involve the sterically protected N_1 and N_2 atoms embedded within the core of the radical. Instead, each methanol hydroxyl group forms two hydrogen bonds with DPPH•. The hydroxyl hydrogens interact primarily with an oxygen atom of the two picryl *o*-NO_2 groups. The corresponding methanol hydroxyl oxygens form bonds with the phenyl hydrogen atoms. Figure 4 also shows that, in the absence of dynamical perturbants, these methanol−DPPH• interactions play a key role in orienting the two phenyl and picryl groups with respect to each other. The interaction of more than four methanol molecules with the DPPH• radical does not significantly influence the orientation of the three DPPH• rings. For example, the extra hydrogen bonds due to two extra methanols are formed with the DPPH• *p*-NO_2 group, as shown in Figure 5. In turn, these extra interactions have very little influence on the positioning of the phenyl and picryl groups with respect to one another. Consequently, this results in very small differences between the computed $a^{iso}(^{14}N_1)$ and $a^{iso}(^{14}N_2)$ values of structures DPPH•−(MeOH)$_4$ and DPPH•−(MeOH)$_6$, given in Table 1. The complex and peripheral nature of these interactions justifies why no direct correlation has been made between the type of solvent and DPPH• reactivity.[13]

The absence of appreciable interactions of the solvent with N_1 and N_2 atoms, where the unpaired electrons mainly resides, explains why DPPH• is a persistent radical. If DPPH• was planar, its $2p_z(N_1)$ and $2p_z(N_2)$ orbitals would be exposed and more reactive. It would be short-lived with a lifetime that is comparable to π-type planar aromatic radicals, such as unsubstituted semiquinones.[52]

3.4. Effects of Restricted Rotations on the Nuclear Hyperfine Coupling Constants. The static model of the DPPH• considered so far has given very good results for the computed $a^{iso}(^{14}N_1)$and $a^{iso}(^{14}N_2)$. However, to add realism to this model, one should take into account rotational averaging when possible.[53,54] Such dynamical effects have been considered and yield excellent results for small organic radicals.[55−57]

The effects of restricted rotations on the **g** tensor components of DPPH• have been investigated, and the resulting computed **g** tensor components are in very good agreement with those determined experimentally.[39] As a continuation of this research, the effects of restricted rotations on the hyperfine tensor components are investigated.

As discussed in section 3.1, the single bonds, C_7-N_2 and $C_{13}-N_2$, formed between the two phenyl and hydrazyl groups will allow these rings to rotate. Nevertheless due to steric hindrance, the phenyl ring rotations will be somewhat restricted. A series of computations were performed to investigate the effect of these restricted rotations on the values of the hyperfine tensors. The $N_1-N_2-C_7-C_8$ dihedral angle, φ_{1278}, was fixed at 0° and the rest of the molecule was geometry optimized to attain a minimum energy conformation. This total energy, $E_{TOT}(\varphi_{1278})$, was noted and the hyperfine tensor components were computed at this newly optimized geometry. The angle, φ_{1278}, was then increased by 5° and the whole process was repeated. This procedure was performed a total of 36 times where φ_{1278} varied between 0° and 175°. The Maxwell−Boltzmann distribution was used, in conjunction with $E_{TOT}(\varphi_{1278})$, to find the probability, $p(\varphi_{1278})$, that the molecule exists in a certain conformation with a specific angle, φ_{1278}. It takes the form

$$p(\varphi_{1278}) = \frac{\exp\left(-\frac{E_{TOT}(\varphi_{1278})}{kT}\right)}{\sum_{\varphi_{1278}=0}^{175} \exp\left(-\frac{E_{TOT}(\varphi_{1278})}{kT}\right)} \quad (1)$$

and was then used to find the averaged hyperfine tensor components via the mean value expression,

$$\langle A_{ij} \rangle = \frac{\sum_{\varphi_{1278}=0}^{175} p(\varphi_{1278}) A_{ij}(\varphi_{1278})}{\sum_{\varphi_{1278}=0}^{175} p(\varphi_{1278})} \quad (2)$$

In the case of the isotropic hyperfine coupling constants eq 2 becomes

$$\langle a^{iso} \rangle = \frac{\sum_{\varphi_{1278}=0}^{175} p(\varphi_{1278}) a^{iso}(\varphi_{1278})}{\sum_{\varphi_{1278}=0}^{175} p(\varphi_{1278})} \quad (3)$$

Figure 6 shows $a^{iso}(^{14}N_1)$, $a^{iso}(^{14}N_2)$ and the corresponding probabilities, $p(\varphi_{1278})$, obtained from eq 1 as a function of the dihedral angle, φ_{1278}. Inspection of Figure 6 shows that $a^{iso}(^{14}N_2)$ varies over a larger range than $a^{iso}(^{14}N_1)$. This is reasonable because N_2, is directly bonded to both phenyl rings and is most affected by their rotations.

The averaged values, $\langle a^{iso}(^{14}N_1) \rangle$ and $\langle a^{iso}(^{14}N_2) \rangle$, as a result of the rotation ranging from 0° to 175° and determined from eqs 1 and 3, at $T = 303.18$ K, are represented by the two horizontal lines in the figure. Table 2 provides a comparison between the DPPH• $a^{iso}(^{14}N_1)$ and $a^{iso}(^{14}N_2)$ values calculated by this rotational averaging method, and the previously known experimental values. As there are no experimental gas phase data for DPPH•, the data used for comparison were taken from DPPH• in benzene. Benzene was chosen because it is nonpolar and its dielectric constant is $\varepsilon = 2.247$. According to the Onsager model, the perturbation of the solute by the solvent generates a reaction field, $\bar{R}$, given by[58]

$$\vec{R} = \frac{2(\varepsilon - 1)\vec{\mu}}{(2\varepsilon + 1)a_0^3} \quad (4)$$

where $\vec{\mu}$ is the molecular dipole moment and a_0 is the solvent cavity radius. Of all the common solvents used to solvate DPPH•, benzene has an ε that is one of the closest to unity. Thus from eq 4 it will also have one of the smallest perturbing effects.

Table 2 lists the $a^{iso}(^{14}N_1)$ and $a^{iso}(^{14}N_2)$ computed with the PCM method. The deviations of the computed values from the experimental ones are given in brackets. Here it is seen that the differences for $a^{iso}(^{14}N_1)$ and $a^{iso}(^{14}N_2)$ are 1.16 and 1.08 G, respectively, which is outside our self-imposed acceptable limits (1.0 G) for these calculations. However, with rotational averaging, the differences drop to +0.17 and −0.79 G. This is a marked improvement, indicating that some rotational averaging is a plausible assumption.

It is worth commenting that in Figure 6 the values of $a^{iso}(^{14}N_1)$ and $a^{iso}(^{14}N_2)$ change abruptly around 115−120°. This is common and a direct consequence of performing a relaxed scan where one internal coordinate is fixed and all others are allowed to change. In this region, the phenyl groups slip by one another and the molecule drops into an energy minimum. The geometry adjusts accordingly and, in turn, the $a^{iso}(^{14}N_1)$ and $a^{iso}(^{14}N_2)$ change sharply.

Although the agreement between the experimental and computed $\langle a^{iso}(^{14}N_1)\rangle$ and $\langle a^{iso}(^{14}N_2)\rangle$ is very good, correlation of the experimental and computed proton isotropic hyperfine coupling constants, $a^{iso}(^1H)$, is much more difficult. This is due to the fact that there are twelve protons and the range of their $a^{iso}(^1H)$ values is very small. The DPPH• radical has C_1 symmetry and is not linear, thus in principle, all its $a^{iso}(^1H)$ values should be different.[14] In practice, the differentiation between all these protons is limited by the spectral resolution

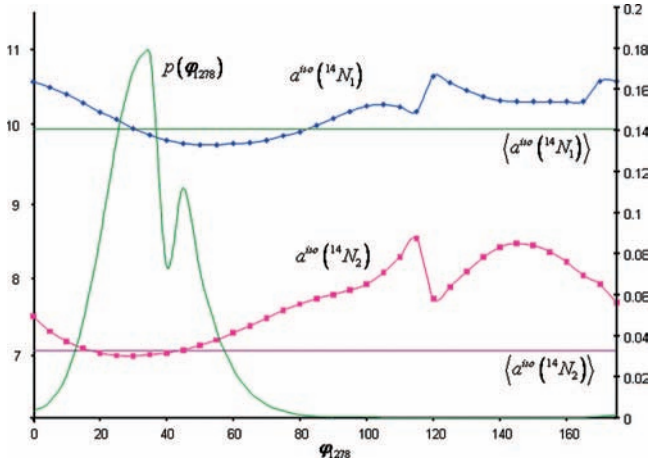

Figure 6. Plot of $a^{iso}(^{14}N_1)$ and $a^{iso}(^{14}N_2)$ points as a function of phenyl ring rotation angle, φ_{1278}. Superimposed on the $a^{iso}(^{14}N_1)$ and $a^{iso}(^{14}N_2)$ curves is the probability plot, $p(\varphi_{1278})$. The *y*-axis on the left represents the a^{iso} scale in Gauss, and that on the right shows the $p(\varphi_{1278})$ range. The horizontal lines represent the rotationally averaged hyperfine coupling constants, $\langle a^{iso}(^{14}N_1)\rangle$ and $\langle a^{iso}(^{14}N_2)\rangle$ obtained from eq 3.

TABLE 2: Rotationally Averaged N_1 and N_2 Isotropic Hyperfine Coupling Constants[a]

	$a^{iso}(^{14}N_1)$	$a^{iso}(^{14}N_2)$
exp/benzene[b]	9.77	7.94
PCM/benzene	10.93 (+1.16)	6.86 (−1.08)
rotationally averaged	9.94 (+0.17)	7.15 (−0.79)

[a] Values in G. [b] From Valgimigli et al.[13]

TABLE 3: Absolute Values of Rotationally Averaged Proton Hyperfine Coupling Constants[a]

$\langle a^{iso}(^1H)\rangle$	calculated	experimental[b]
$\langle a^{iso}(^1H_{17})\rangle$	0.42	0.67
$\langle a^{iso}(^1H_5)\rangle$	0.86	0.75
$\langle a^{iso}(^1H_{16})\rangle$	0.87	0.75
$\langle a^{iso}(^1H_{11})\rangle$	0.91	1.0
$\langle a^{iso}(^1H_9)\rangle$	0.97	1.0
$\langle a^{iso}(^1H_{18})\rangle$	1.04	1.0
$\langle a^{iso}(^1H_{15})\rangle$	1.07	1.0
$\langle a^{iso}(^1H_{14})\rangle$	1.24	1.0
$\langle a^{iso}(^1H_3)\rangle$	1.86	1.9
$\langle a^{iso}(^1H_{10})\rangle$	1.95	1.9
$\langle a^{iso}(^1H_{12})\rangle$	2.07	2.0
$\langle a^{iso}(^1H_8)\rangle$	2.09	2.0

[a] Values in G. [b] Experimental values of **DPPH•** in mineral oil.[15−17]

and the inherent line widths. In addition, rotational averaging will also be a contributing factor. Rotational averaging of the twelve isotropic proton coupling constants has been performed. The resulting $\langle a^{iso}(^1H)\rangle$ are listed in Table 3. In this table one attempts to order the calculated $\langle a^{iso}(^1H)\rangle$ values in ascending order and tentatively assign the corresponding experimental values. It is comforting that the magnitude of these computed and experimental $\langle a^{iso}(^1H)\rangle$ values are all in the range 0−2.0 G. Assuming that the groupings of the twelve protons are correct, the maximum difference between the rotationally averaged and experimental values is 0.25 G. Although this is excellent numerical accuracy, further pulsed and solid state ENDOR experiments are needed to unequivocally assign the total hyperfine tensor components from which the corresponding $a^{iso}(^1H)$ values can be determined.

4. Summary and Conclusions

The DPPH• geometry obtained by optimization, and shown in Figure 1, is found to be nonplanar and close to that determined by X-ray crystallography. The electronic structure calculations reveal that a large portion of unpaired electron is situated on the central N_1 and N_2 atoms. However, the rest of its spin density is delocalized over the entire molecule. Figure 3 further shows that the SOMO has partial π double bond character spanning its N_2, N_1, and C_1 atoms.

The DPPH• hyperfine coupling constants are calculated using hybrid density functionals and the EPR-II double-ζ basis sets. The net spin density at N_1 is calculated to be greater than that at N_2. This corroborates the experimental finding that $a^{iso}(^{14}N_1)$is greater than $a^{iso}(^{14}N_2)$.

The calculations were initially performed while considering the molecule in a gas phase, and then solvent effects were introduced. In the case of methanol, solvent interactions were estimated in three ways: the first and second were using the PCM and COSMO methods and the third was to geometry optimize the DPPH• molecule when it is hydrogen bonded to an increasing number of methanol molecules, ranging from 1 to 6. The interactions of the first four methanol molecules with the picryl *ortho*-nitro groups of DPPH• have an important effect on the orientation of the two phenyl rings with respect to the picryl group. The interaction of extra methanol molecules with DPPH• does not appreciably influence the orientation of the three rings and the hyperfine coupling constants. The lack of direct interactions between the solvent molecules and the $N_1{=}N_2$ functional group, where the unpaired electron is mainly located, explains why DPPH• is a stable radical.

The effects of restricted rotations, along the N_2-phenyl single bonds, on the hyperfine coupling constants have been investigated, and the resulting averaged $\langle a^{iso}(^{14}N_1)\rangle$ and $\langle a^{iso}(^{14}N_2)\rangle$ are in very good agreement with the experimental values. For example, rotational averaging of $a^{iso}(^{14}N_1)$ and $a^{iso}(^{14}N_2)$ drops the difference between the theory and experiment to +0.17 and −0.79 G, respectively. This significant improvement suggests that rotational averaging is a reasonable assumption.

In the case of the twelve hydrogen atoms, the computed and experimental value of the rotationally $\langle a^{iso}(^{1}H)\rangle$ all lie in the range 0−2.0 G. The accuracy of the calculations is excellent where the maximum difference between the rotationally averaged and experimental values is only 0.25 G.

Overall, the computations in this paper are in very good agreement with experiment. This proves that the hybrid density functional electronic structure results depict a realistic picture of the magnetic properties, structure, and spin density distribution of this large 41-atom molecule.

Acknowledgment. This article is dedicated to Professor Naresh S. Dalal, for his long outstanding contributions in EPR and ENDOR spectroscopy. S.M.M. thanks the Natural Sciences and Engineering Research Council of Canada for financial support in the form of operating (Discovery) grants. J.S. acknowledges the University of New Brunswick for a predoctoral assistantship. We are grateful to Professor Frank Neese for the use of his ORCA suite of programs.

References and Notes

(1) Goldschmidt, S.; Renn, K. *Ber. Deutsch. Chem. Ges. B* **1922**, *55B*, 628–643.
(2) Lohe, J.; Elia, G. *Acta Chem. Scand.* **1958**, *12*, 1535.
(3) Livingston, R.; Zeldes, H; Taylor, E. H. *Discuss. Faraday Soc.* **1955**, *19*, 166–173.
(4) Krzystek, J.; Sienkiewicz, A.; Pardi, L.; Brunel, L. C. *J. Magn. Reson.* **1997**, *125*, 207–211.
(5) Kolaczkowski, S. V.; Cardin, J. T.; Budil, D. E. *Appl. Magn. Reson.* **1999**, *16*, 293–298.
(6) Ordoudi, S. A.; Tsimidou, M. Z.; Vafiadis, A. P.; Bakalbasis, E. G. *J. Agric. Food Chem.* **2006**, *54*, 5736–5768.
(7) Hutchison, C. A., Jr.; Pastor, R. C.; Kowalsky, A. G. *J. Chem. Phys.* **1952**, *20*, 534–535.
(8) Deal, R. M.; Koski, W. S. *J. Chem. Phys.* **1959**, *31*, 1138–1139.
(9) Holmberg, R. W.; Livingston, R.; Smith, W. T., Jr. *J. Chem. Phys.* **1960**, *33*, 541–546.
(10) Gamo, K.; Masuda, K.; Yamaguchi, J.; Kakitani, T. *J. Phys. Soc. Jpn.* **1965**, *20*, 1730.
(11) Gubanov, V. A.; Koryakov, V. I.; Chirkov, A. K. *J. Magn. Reson. (1969−1992)* **1973**, *9*, 263–274.
(12) Garif'yanov, N. S.; Il'yasov, A. V.; Yablokov, Yu. *Dokl. Akad. Nauk SSSR* **1963**, *149*, 876–879.
(13) Valgimigli, L.; Ingold, K. U.; Lusztyk, J. *J. Org. Chem.* **1996**, *61*, 7947–7950.
(14) Mattar, A. M. *Chem. Phys. Lett.* **1998**, *287*, 608–612.
(15) Dalal, N. S.; Kennedy, D. E.; McDowell, C. A. *J. Chem. Phys.* **1973**, *59*, 3403–3410.
(16) Dalal, N. S.; Kennedy, D. E.; McDowell, C. A. *J. Chem. Phys.* **1974**, *61*, 1689–1697.
(17) Dalal, N. S.; Kennedy, D. E.; McDowell, C. A. *Chem. Phys. Lett.* **1975**, *30*, 186–189.
(18) Feller, D.; Davidson, E. R. *J. Chem. Phys.* **1984**, *80*, 1006–1017.
(19) Feller, D.; Glendening, E. D.; McCullough, E. A., Jr.; Miller, R. J *J. Chem. Phys.* **1993**, *99*, 2829–2840.
(20) Mattar, S. M.; Hamilton, W. D.; Kingston, C. T. *Chem. Phys. Lett.* **1997**, *271*, 125–132.
(21) Neese, F. *J. Chem. Phys.* **2003**, *119*, 9428–9443.
(22) Foresman, J. B.; Frisch, A. *Exploring Chemistry With Electronic Structure Models*; Gaussian, Inc.: Pittsburgh, PA, 1996.
(23) Improta, R.; Barone, V. *Chem. Rev.* **2004**, *104*, 1231–1254.
(24) Adamo, C.; Barone, V. *Chem. Phys. Lett.* **1997**, *274*, 242–250.
(25) Mattar, S. M.; Stephens, A. D. *Chem. Phys. Lett.* **1999**, *306*, 249–255.
(26) Adamo, C.; di Matteo, A.; Rey, P.; Barone, V. *J. Phys. Chem. A* **1999**, *103*, 3481–3488.
(27) Di Matteo, A.; Adamo, C.; Cossi, M.; Barone, V.; Rey, P. *Chem. Phys. Lett.* **1999**, *310*, 159–165.
(28) Mattar, S. M.; Stephens, A. D. *Chem. Phys. Lett.* **2000**, *319*, 601–610.
(29) *Recent Advances in Density Functional Methods*; Barone, V., Chong, D. P., Ed.; World Scientific Publishing Company: Singapore, 1996.
(30) Mattar, S. M.; Stephens, A. D. *Chem. Phys. Lett.* **2001**, *347*, 189–198.
(31) Mattar, S. M.; Stephens, A. D. *J. Phys. Chem. A* **2000**, *104*, 3718–3732.
(32) Mattar, S. M.; Stephens, A. D. *Chem. Phys. Lett.* **2000**, *327*, 409–419.
(33) Neese, F. *Magn. Reson. Chem.* **2004**, *42*, S187–S198.
(34) Walter, R. *J. Am. Chem. Soc.* **1966**, *88*, 1930.
(35) Gubanov, V. A.; Perelyaeva, L. A.; Chirkov, A. K.; Matevosian, R. O. *Theor. Chim. Acta (Berl.)* **1970**, *18*, 177–183.
(36) Williams, D. E. *J. Am. Chem. Soc.* **1967**, *89*, 4280–4287.
(37) Kiers, C. T.; de Boer, J. L.; Olthof, R. A.; Spek, A. L. *Acta Crystallogr. B* **1976**, *32*, 2297.
(38) Boucherle, J. X.; Gillon, B.; Maruani, J.; Schweizer, J. *Acta Crystallogr. C* **1987**, *43*, 1769–1773.
(39) Mattar, S. M.; Sanford, J. *Chem. Phys. Lett.* **2006**, *425*, 148–153.
(40) Neese, F. *ORCA - an ab initio, density functional and semiempirical program package*, version 2.6−4.0; University of Bonn: Bonn, Germany, 2007.
(41) Frish, M. A.; et al. *Gaussian03*, revision D.02; Gaussian Inc.: Wallingford, CT, 2004.
(42) Perdew, J. P.; Burke, K.; Ernzerhof, M. *Phys. Rev. Lett.* **1997**, *78*, 1396.
(43) Adamo, C.; Barone, V. *J. Chem. Phys.* **1999**, *110*, 6158–6170.
(44) Barone, V.; Cossi, M.; Tomasi, J. *J. Chem. Phys.* **1997**, *107*, 3210–3221.
(45) Cossi, M.; Scalmani, G.; Rega, N.; Barone, V. *J. Chem. Phys.* **2002**, *117*, 43–54.
(46) Klamt, A.; Jonas, V.; Burger, T.; Lohrenz, J. C. W. *J. Phys. Chem. A* **1998**, *102*, 5074–5085.
(47) Mattar, S. M.; Emwas, A. H.; Stephens, A. D. *Chem. Phys. Lett.* **2002**, *363*, 152–160.
(48) Mattar, S. M.; Stephens, A. D.; Emwas, A. H. *Chem. Phys. Lett.* **2002**, *352*, 39–47.
(49) Mattar, S. M.; Emwas, A. H. *Chem. Phys. Lett.* **2003**, *368*, 724–731.
(50) Mattar, S. M. *J. Phys. Chem. B* **2004**, *108*, 9449–9455.
(51) Asher, J. R.; Doltsinis, N. L.; Kaupp, M. *J. Am. Chem. Soc.* **2004**, *126*, 9854–9861.
(52) Mattar, S. M.; Sammynaiken, R.; Stephens, A. D. *J. Phys. Chem.* **1997**, *101*, 8227.
(53) Sullivan, P. D. *J. Phys. Chem.* **1971**, *75*, 2195.
(54) Eloranata, J.; Suontamo, R.; Vuolle, M. *J. Chem. Soc., Faraday Trans.* **1997**, *93*, 3313–3317.
(55) Brancato, G.; Rega, N.; Barone, V. *J. Am. Chem. Soc.* **2007**, *129*, 15380–15390.
(56) Pavone, M.; Cimino, P.; Crescenzi, O.; Sillanpaeae, A.; Barone, V. *J. Phys. Chem. B* **2007**, *111*, 8928–8939.
(57) Zerbetto, M.; Carlotto, S.; Polimeno, A.; Corvaja, C.; Franco, L.; Toniolo, C.; Formaggio, F.; Barone, V.; Cimino, P. *J. Phys. Chem. B* **2007**, *111*, 2668–2674.
(58) Onsager, L. *J. Am. Chem. Soc.* **1936**, *58*, 1486.

JP806919K